THE INTERNATIONAL JOURNAL OF MEDICAL ROBOTICS AND COMPUTER ASSISTED SURGERY
Int J Med Robotics Comput Assist Surg 2010; **6**: 334–342.
Published online 7 July 2010 in Wiley Online Library (wileyonlinelibrary.com) **DOI:** 10.1002/rcs.340

ORIGINAL ARTICLE

Estimation and filtering of physiological tremor for real-time compensation in surgical robotics applications

K. C. Veluvolu[1]*
W. T. Ang[2]

[1]*School of Electronics Engineering, College of IT Engineering, Kyungpook National University, Daegu, South Korea*

[2]*School of Mechanical and Aerospace Engineering, Robotics Research Centre, Nanyang Technological University, Singapore*

*Correspondence to: K. C. Veluvolu, School of Electronics Engineering, College of IT Engineering, Kyungpook National University, Daegu, South Korea.
E-mail: veluvolu@ee.knu.ac.kr

Accepted: 30 May 2010

Abstract

Background Physiological tremor is the main cause of imprecision in microsurgical procedures/robotics applications. Existing methods, such as weighted-frequency Fourier linear combiner (WFLC), rely on estimating the tremor under the assumption that it has a single dominant frequency. This paper focuses on developing a new algorithm for accurate tremor filtering in real time.

Methods A study conducted on several novice subjects and microsurgeons showed the tremor to contain several dominant frequencies in a band, rather than a single dominant frequency. Based on the tremor characteristics, a new algorithm band-limited multiple Fourier linear combiner (BMFLC) has been developed to estimate a band of signals with multiple dominant frequencies. A separation procedure to separate the intended motion/drift from the tremor portion is also discussed.

Results A simulation study was first conducted to validate the theoretical development on recorded tremor data. The experimental set-up was designed to study the real-time performance of the proposed algorithm. Tremor sensing using accelerometers is also discussed, with the proposed algorithm. Our experiments showed that the developed BMFLC algorithm had an average tremor compensation of 64% compared to 43% for the WFLC algorithm in real-time for one degree of freedom (1-DOF) cancellation of tremor.

Conclusions The BMFLC algorithm can be applied for the three axes separately and 3-DOF cancellation of tremor can be achieved. Further research is required to deal with complex gestures involved during microsurgery.

Keywords tremor filtering; real-time compensation; computer-assisted surgery; signal processing

Introduction

Physiological tremor leads to an intolerable imprecision of surgical procedure, e.g. for vitroretinal surgery, which requires a positioning accuracy of about 10 μm (1). In (2) it was shown that the tremor corrupts the voluntary motion, causing an unwanted disturbance or noise. Tremor is an involuntary human hand motion, can be approximated by a sinusoidal

movement (3) and exists in all human motion. Tremor lies in the band 6–15 Hz, with an amplitude of 100 μm in each principal axis (3–8).

Tremor filtering and estimation has received significant attention over the last decade (2,4,9–13). The majority of the existing techniques rely on low-pass filtering approaches to cancel the tremor. In (13) the tremor was treated as noise and a digital filter was employed for suppression. In (14) a real-time algorithm to predict physiological tremor using an AR model was developed. Although linear filters are successful in compensating tremor, the inherent time delay (15) ia a major drawback where zero-phase filtering is required. In (16) it was shown that delays as small as 30 ms may degrade performance in human–machine control applications. Effective tremor compensation requires zero phase lag in the filtering process, so that the filtered tremor signal can be used to generate an opposing motion to tremor in real time.

To overcome the problems caused by delays in low-pass filtering, adaptive filtering approaches have been developed (17–19). These are well suited for tremor estimation, as the filter (17) can adapt to the changes in frequency and amplitude of the tremor signal. The adaptation process is achieved using a least mean square (LMS) optimization algorithm. Fourier linear combiner (FLC) (18,19) is an adaptive filter that forms a dynamic truncated Fourier series model of an input signal. The FLC operates by adaptively estimating the Fourier coefficients of the known frequency model according to the LMS algorithm. The FLC effectively estimates and cancels periodic interference of known frequency. Weighted-frequency Fourier linear combiner (WFLC) is an adaptive algorithm which models any quasi-periodic signal as a modulating sinusoid and tracks its frequency, amplitude and phase. WFLC incorporates frequency adaptation procedure into FLC. The main drawback of WFLC lies in tracking signals with modulated frequencies, e.g. subjects with essential tremor (20). Any presence of high-frequency noise affects the frequency adaptation and compels the use of pre-filtering (band-pass filter), which introduces delay into the filtering process. A similar algorithm was also developed in continuous time for rejection of sinusoidal signals with unknown frequencies (21).

Tremor compensation for robotics-assisted surgical procedures has received significant attention (22–24). Physiological tremor presents a huge challenge, due to the high-frequency band and its application in real time. In (22,23) a robotic hand-held instrument (Micron) to cancel the surgeon's physiological tremor in vitreoretinal microsurgery was implemented. The tip of the instrument will be unaffected by the tremor motion of the surgeon. The error compensation control loop has to be executed in real time, i.e. the system has to sense the motion of interest, distinguish between voluntary and undesired components and take the appropriate action (hardware or software) to nullify the erroneous part in one sampling cycle. This approach will only work when there is a distinctive frequency separation between the desired and unwanted motion. For example, the dominant frequency of physiological hand tremor lies in the band 6–15 Hz, while the hand movement of the surgeon during microsurgery is almost always <0.5 Hz. Most of the earlier techniques discussed are not be applicable for robotics-related tremor cancellation due to the involvement of accelerometers, which only provide acceleration of the tremor motion. The main purpose of this research was to improve tremor filtering and to provide drift-free tremor in the displacement domain. The WFLC algorithm in general adapts to a single frequency present in the incoming signal. For the case of a tremor signal modulated by two frequencies close in the spectral domain, the performance of WFLC will be degraded.

A study was conducted on several novice subjects and microsurgeons to study tremor characteristics. Based on the study, a new algorithm, BMFLC (25), was developed to estimate the tremor. The proposed algorithm has constant frequency weights in a given band and can be implemented easily. As the frequency weights are constants, the tremor sensed through accelerometers can be converted to the displacement domain through analytical integration. Experiments were conducted using existing and proposed algorithms to evaluate the real-time tremor cancellation using piezo-electric actuators. In simulations and experiments, the proposed method performed better than the WFLC.

Materials and Methods

Tremor characteristics

In this section, we analyse the tremor profiles of various subjects to research on the tremor frequencies and bandwidths. Earlier studies (3,4,6,8) have indicated that physiological tremor frequency has a single dominant frequency in the 6–15 Hz band, with an amplitude of 100 μm (rms) in the x, y and z directions.

To study various aspects of tremor, an earlier developed micro-motion-sensing system (M^2S^2) (26,27) was employed. The M^2S^2 (Figure 1) consists of a pair of orthogonally placed position sensitive detectors (PSDs) and an infra-red (IR) diode to track the 3D displacement of the tip of the microsurgical instrument in real time. The IR diode is used to illuminate the workspace. A ball is attached to the tip of an intra-ocular shaft to reflect IR rays onto the PSDs. Instrument tip position is then calculated from the centroid position of the light falling on the PSDs. The resolution, minimum accuracy and sampling rate of the M^2S^2 are 0.7 μm, 98% and 250 Hz, respectively (26).

The tremor data were recorded from six healthy subjects (four male, two female) and 10 (six male, four female) microsurgeons for analysis. Two types of tests were performed on the subjects: (a) stationary; and (b) tracking tests. In the stationary tests, subjects were instructed to point the laser light at the centre point of

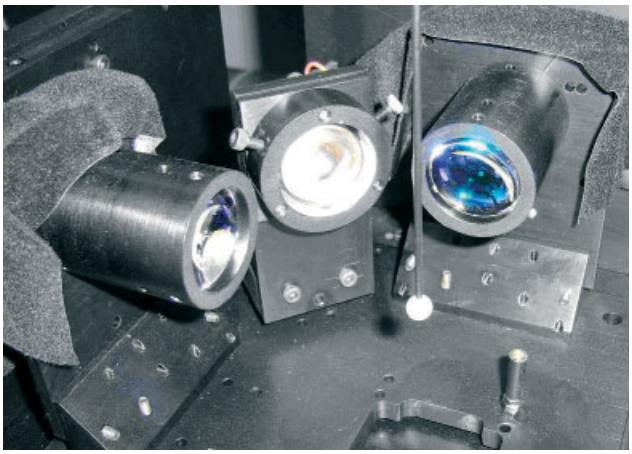

Figure 1. M2S2 set-up

the platform. Tracking tests were path-dependent tests and the subjects were asked to trace the circumference of a circular path on the platform at a speed realistic for surgical micromanipulation tasks. The absolute FFT spectrum for two surgeons and two novice subjects are shown in Figure 2, with stationary and tracing tests. For simplicity, only the tremor in the z axis is shown. The data collected from the surgeons and novice subjects (six normal subjects, 10 surgeons) in our experiments showed that there existed a bandwidth of 2–3 Hz with several peaks in the band. Our experiments also showed that typically several dominant tremor frequencies are present.

The two tests were conducted to verify whether the characteristics were affected when there was an intended motion involved in the act. However, most subjects displayed similar characteristics in tremor bandwidth between stationary and tracking tests, while the amplitude of tremor was slightly lower while performing tracking tests. Statistical analysis showed that for microsurgeons, mean ± SD for the band and bandwidth were [9.33 (± 0.6) – 11.6 (± 0.65)] Hz and 2.4 (± 0.51) Hz, respectively. For the novice subjects, mean ± SD for the band and bandwidth were [7.6 (± 0.42) – 10.3 (± 0.44)] Hz and 2.7 (± 0.44) Hz, respectively. The characteristics including the gender are given in more detail in Table 1. The tremor frequency of the surgeons was about 2 Hz higher than for the novice subjects. The bandwidth of the surgeons was 0.3 Hz smaller than for the novice subjects and the tremor amplitude of the surgeons was a factor of about 2–3 lower than that for the novices. It can be noted that the surgeons exhibited a certain level of control on their tremor under test (and operation) conditions.

Table 1 shows the maximum and root mean square of the tremor amplitudes. Awareness of the tests and procedures likely affected the tremor bands, as the surgeons were also able to control the tremor amplitude. For some novice subjects, although the band of

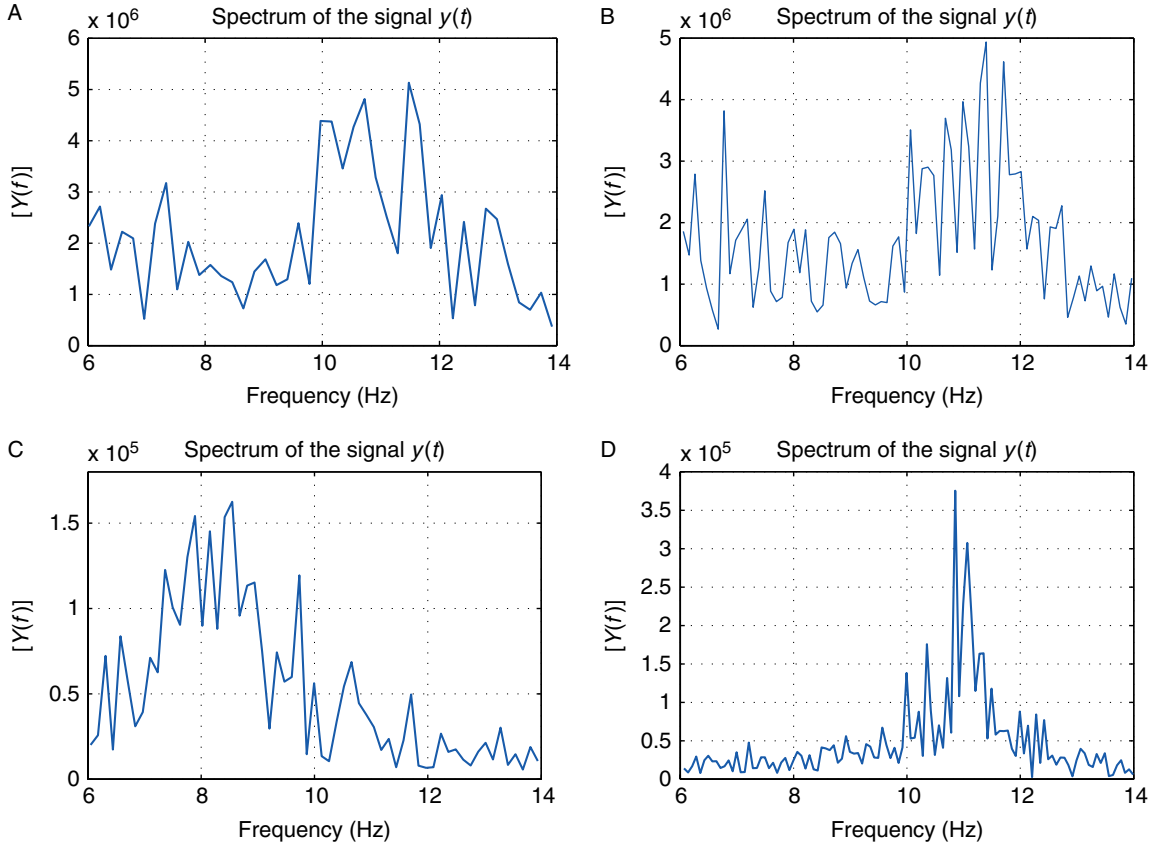

Figure 2. Amplitude FFT response of two surgeons and two novice subjects in the band 6–14 Hz. (A) Surgeon 1 (stationary test); (B) surgeon 5 (tracking test); (C) subject 4 (tracking test); (D) subject 5 (stationary test)

Table 1. Tremor characteristics

Novice subject/surgeon	Average frequency band	Average tremor amplitude	
		RMS (μm)	Max (μm)
4 Novice subjects (male)	7.8–10.5	28.4	42.6
2 Novice subjects (female)	7–9.8	31.4	44.2
6 Micro-surgeons (male)	9.2–11.5	18.7	26.4
4 Micro-surgeons (female)	9.6–12.4	16.1	25.2

frequencies had a peak, they were well distributed within a range of 3–4 Hz bandwidth.

In an earlier analysis (20), subjects with Parkinson's tremor displayed a band with a single peak, whereas subjects with essential tremor exhibited a bandwidth of 3–4 Hz. Most healthy subjects have a distributed band with many frequencies, in contrast to Parkinson's patients, who have a single dominant frequency. The amplitude of the single peak in FFT of Parkinson's tremor is very high compared to the multiple peaks of healthy subjects. To generalize our development in this paper, we consider the band of tremor to be in the range 6–14 Hz.

Band-limited multiple-Fourier linear combiner

The presence of multiple peaks in the FFT spectrum is the result of modulation of multiple frequency components in tremor. The existing FLC methods and WFLC algorithms in general adapt to a single frequency present in the incoming signal. In the case of tremor signals modulated by multiple frequencies close in the spectral domain, the performance of WFLC will be degraded. In such cases the frequency adaption process of the WFLC can never be stabilized and accurate estimation of the tremor signal cannot be attained. If the frequency variations are fast, the performance of WFLC will be degraded. Even the presence of two or three frequencies closely spaced in the spectral domain can adversely affect the performance of WFLC, e.g. 8.2 Hz and 8.4 Hz signals produce a modulated wave containing both the frequencies. In this case, the frequency adaption process of the WFLC can never be stabilized and accurate estimation of the tremor signal cannot be attained. Any presence of high frequency noise can change the adaptation process of the algorithm. To overcome these aspects, a method has been developed to estimate the modulated signals in a given band of interest.

Based on our study in earlier section, without loss of generality, we consider the tremor signal to be distributed in the band $\omega_1 - \omega_n$ and then divide the frequency band of interest into n finite divisions, as shown in Figure 3B. For the estimation of the unknown tremor signal, we then choose a series comprising sine and cosine components to form a band-limited multiple-Fourier linear combiner (BMFLC):

$$y_k = \sum_{r=1}^{n} a_{rk} \sin(\omega_r k) + b_{rk} \cos(\omega_r k) \tag{1}$$

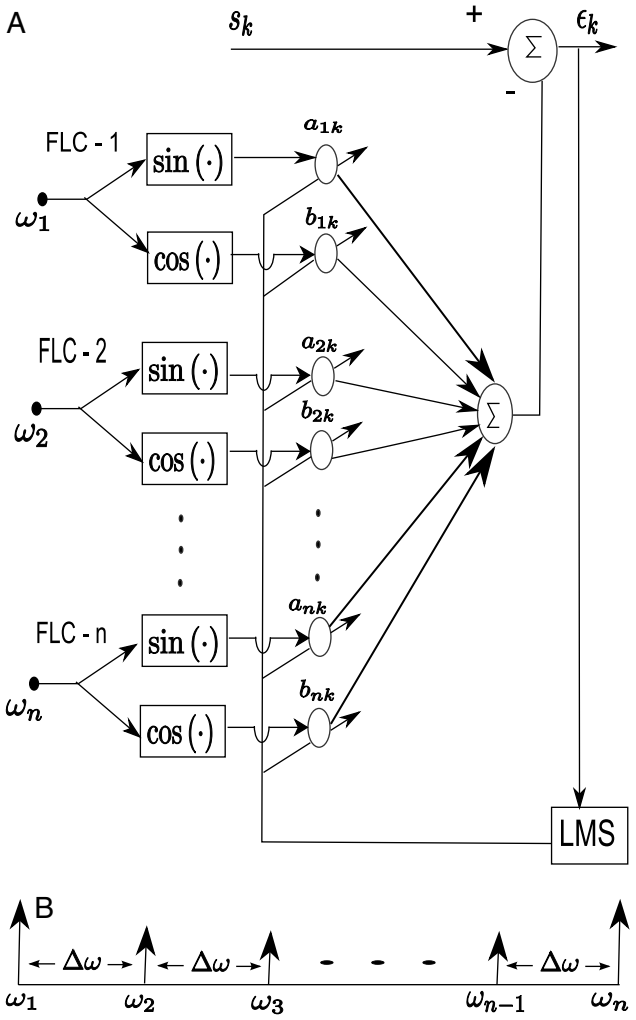

Figure 3. (A) BMFLC architecture; (B) frequency distribution for multiple FLCs

where y_k denotes the estimated signal at sampling instant k. a_{rk} and b_{rk} represent the adaptive weights corresponding to the frequency ω_r at instant k. The following series only considers n fundamental frequencies in the band. The division of the band, step size $\Delta\omega$ (in Figure 3B) and selection of the fundamental frequencies will be discussed in the later part of the section.

We then adopt the LMS algorithm (17) to adapt the weights a_{rk}, b_{rk} in equation (1) to the incoming unknown signal. The architecture of the proposed algorithm is shown in Figure 3A. The algorithm can be stated as follows:

$$\mathbf{x}_k = \left\{ \begin{array}{cccc} [\sin(\omega_1 k) & \sin(\omega_2 k) & \cdots & \sin(\omega_n k)]^T \\ [\cos(\omega_1 k) & \cos(\omega_2 k) & \cdots & \cos(\omega_n k)]^T \end{array} \right\} \tag{2}$$

$$y_k = \mathbf{w}_k^T \mathbf{x}_k \tag{3}$$

$$\varepsilon_k = s_k - y_k \tag{4}$$

$$\mathbf{w}_{k+1} = \mathbf{w}_k + 2\,\mu \mathbf{x}_k \varepsilon_k \tag{5}$$

where $\mathbf{w}_k = [a_{1k} \quad \cdots \quad a_{nk} \quad b_{1k} \quad \cdots \quad b_{nk}]^T$ and $\mathbf{x}_k$ are the adaptive weight vector and reference input vector, respectively, s_k is the reference signal, ε_k represents the

error term and μ and is an adaptive gain parameter. Input signal amplitude and phase are estimated by the adaptive vector $\mathbf{w}_k$. The FLC is inherently zero phase (18) and has an infinite null (17). The algorithm can be viewed as multiple notch filters, with the width of each notch being directly proportional to μ (28).

As shown in the architecture, n-FLCs are combined to form the BMFLC to estimate band-limited signals. FLC and WFLC are designed to estimate periodic signals of a single fundamental frequency. Comparing with FLC, we remove the harmonics in FLC, i.e. we have $M = 1$ in (18), with multiple frequency components representing multiple FLCs. With the LMS optimization algorithm, the corresponding weights of the individual frequencies in n-FLCs adapt to their respective frequency components present in the band of interest. The adaptive gain parameter μ can be chosen to have fast convergence without losing stability. The stability of the algorithm can be established similar to (18). As the weights are fixed in the algorithm, any modulated signals can be estimated in the given band with the amplitude weights, whereas WFLC requires frequency adaptation and the amplitude estimate cannot be accurate unless the frequency weight stabilizes. So WFLC cannot track signals with rapid changes in frequency or modulated signals with multiple frequencies.

The success of tremor compensation in surgical robotic applications also depends on reliable separation of intended motion/drift from tremor signals. To deal with this problem, in our proposed algorithm a bias weight (17) with adaptive gain is introduced to separate the intended motion/drift (low frequency component) from the tremor signal. This avoids the need for pre-filtering (low-pass filter) that is required in WFLC. The algorithm can be modified by adding an extra term, $a_0 > 0$, to the reference vector $\mathbf{x}_k^* = [\,\mathbf{x}_k^T \quad a_{0k}\,]^T$ and adaptive weight vector $\mathbf{w}_k^* = [\,\mathbf{w}_k^T \quad a_{0k}\,]^T$. The intended motion/drift component can obtained as $I(k) = \mathbf{w}_k^*(2l+1,:)/a_{0k}$.

The frequency band selection depends on the subjects, as concluded in our research study. For estimation without any prior knowledge on the subject, a band of 6–14 Hz can be selected. With prior knowledge of the subject tremor, a narrow band can be selected. For surgeons, a band of 9–13 Hz is more suited for estimation with BMFLC, based on our study conducted earlier. If the tremor band of the surgeon is analysed, the band can be adjusted based on the prior analysis.

The accuracy of estimation depends on the frequency spacing $\Delta\omega$. A small $\Delta\omega$ will increase the number of fundamental frequencies (and weights) and the estimation process will be highly accurate. A value of 0.1–0.5 for $\Delta\omega$ is optimum for estimation of tremor to obtain an accuracy of 96–98%. A very small $\Delta\omega$ will increase the number of weights and the number of parameters in the model can no longer be handled in real time. Also, with increase in the number of weights, the susceptibility of the filtering process to high-frequency noise also increases. Hence it is recommended to choose a bandwidth of 2–3 Hz with proper spacing. Our study showed that a frequency spacing of 0.1 Hz will result in good estimation accuracy.

Table 2. Comparison of WFLC and BMFLC on synthesized signal

Frequency		WFLC		BMFLC	
f_1	f_2	$\hat{\varepsilon}$ (RMS)	Compensation (%)	ε (RMS)	Compensation (%)
8	8	0.0135	98.7	0.117	96.16
8	9	0.765	75.06	0.116	96.17
8	10	1.22	59.83	0.116	96.19
6	12	2.33	23.48	0.124	95.91

Results

Simulation study and analysis

To evaluate the performance of WFLC and BMFLC on modulated signals, we chose a modulating sinusoidal signal with two frequencies as follows:

$$s_k = 3.5\sin(2\pi f_1 t) + 2.5\cos(2\pi f_2 t)$$

The following parameters were set for the WFLC algorithm: $\mu_0 = 0.017$, $\mu = 0.012$, $\hat{\mu} = 1 \times 10^{-5}$, $\omega_{0_1} = 0$. For the proposed algorithm, the parameters are set to be $\mu = 0.01$, $\Delta\omega = 0.1$, $\omega_1 = 2\pi \times 6$ and $\omega_n = 2\pi \times 14$. For various values of f_1 and f_2 the performance characteristics of the WFLC and BMFLC are shown in Table 2. As the frequency gap between f_1 and f_2 widens, WFLC fails to adapt to the modulated signal. The proposed algorithm maintains a constant compensation, irrespective of the frequency of the signals, but when both the frequencies are equal ($f_1 = f_2 = 8$) the WFLC performs slightly better than the proposed algorithm.

To further evaluate the algorithm, it was tested on tremor recordings of the subjects/surgeons. The tremor data of subjects was band pass-filtered with pass bands 6–14 Hz. Band pass-filtered signal is essential for estimation with WFLC (7). The performance of WFLC is shown in Figure 4; only a small portion of the signal is presented for clarity. Figure 5 shows the estimation performance of BMFLC. In comparison, the inaccuracy in estimation can be seen in WFLC when there are amplitude and frequency modulations.

To further quantify the performance, the analysis was also conducted on the tremor data of six novice subjects and 10 surgeons and the average compensation is tabulated in Table 3. The proposed approach performed better than the WFLC method with real tremor data.

Experimental set-up

An accelerometer board (DE-ACCM2G, Dimension Engineering), containing a ADXL322 dual axis accelerometer and dual rail-to-rail operational amplifier buffers were

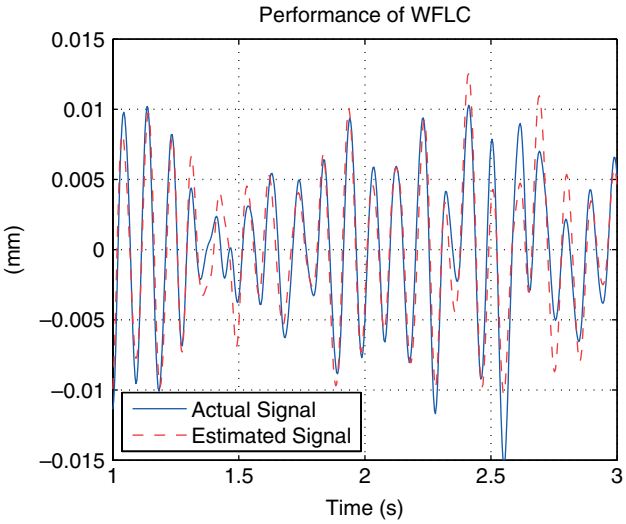

Figure 4. Performance of BMFLC, surgeon no. 5

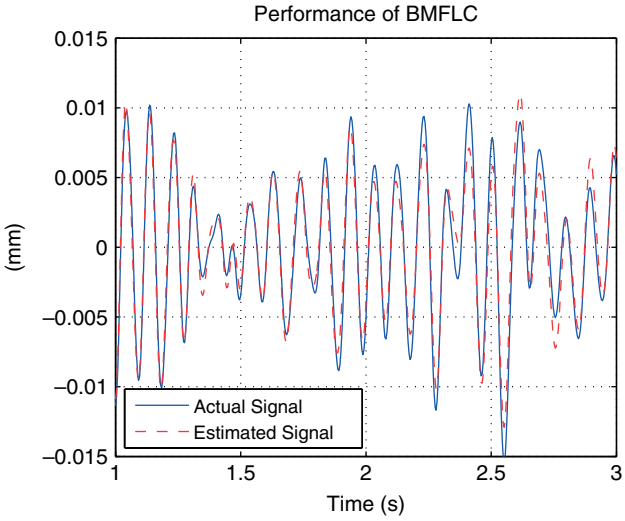

Figure 5. Performance of WFLC, surgeon no. 5

Table 3. Performance of WFLC and BMFLC on tremor

	Average compensation (%)	
Subjects	WFLC	BMFLC
Novice subjects (4 M, 2 F)	64.2	93.5
Surgeons (6 M, 4 F)	56.4	87.8

M, male; F, female.

employed for the experiment. A QNX real-time operating system was used to acquire the accelerometer output data in real time. The sampling rate of the DAQ card [PD2-MF-150, United Electronic Industries (UEI)] was set to 120 kHz. Interruption was performed every 0.5 ms and its timing period was created through a QNX timer. Therefore, the acquired data were made available to the user program at a rate of 2 kHz (1/0.5 ms). The 60 samples (120k/2000) in each interruption time were averaged to get one sample in order to remove unwanted high-frequency noise in the measurements. We modelled the accelerometer by a quadratic function, using least squares fit. The accelerometer was moved up and down at a frequency of 8 Hz with known amplitude, using a nanopositioning system P-561.3CD from Physik Instrumente (PI). The peak-to-peak distance of the motion was 100 μm. This displacement information was used to calculate actual acceleration by double differentiation. The voltage reading from the accelerometer was converted to acceleration by means of a quadratic function.

The main purpose of this research was to develop smart surgical device, such as Micron (7,23), with accelerometers to sense the tremor and cancel in real time during microsurgery. The cancellation of tremor was performed through piezoelectric actuators in the displacement domain. As the input to the piezoelectric actuators was required in the displacement domain, the algorithm needed to provide an accurate estimate of displacement. As accelerometers only provide acceleration measurements, numerical integration was generally performed to obtain the position information. Due to the presence of noise and DC bias, the integration drift grew quadratically over time after double integration (29). The drift was unavoidable, and its presence corrupted the position information.

To overcome the drift, we applied our proposed algorithm in the acceleration domain to obtain the acceleration of the tremor signal (29). As the frequency components remain constant in BMFLC, double integration of equation (1) yields:

$$\int\int y_k = -\sum_{r=1}^{n}\left[\frac{a_{rk}}{(\omega_r)^2}\sin(\omega_r k) + \frac{b_{rk}}{(\omega_r)^2}\cos(\omega_r k)\right] \quad (6)$$

As the algorithm provides the weight vectors of all the sine and cosine components, the non-drifting position information can be obtained with (6) without a need for numerical integration.

Real-time implementation

Compensation of the tremor motion needs to be performed in real-time systems and hence, to support this, a QNX Neutrino Real-time Operating System and PD2MF Series PowerDAQ data acquisition boards were used. A known positive disturbance of 8 Hz with RMS motion of 33.3 μm was given as input. As shown in Figure 6A, the disturbance motion was sensed by the accelerometer inertial measurement unit (IMU). We use (6) to obtain the non-drifting position measurement from the acceleration data. The tremor disturbance was provided by a nanopositioning system (P-561.3CD, Physik Instrumente). The displacement readings after the compensation through the piezoelectric-driven mechanism were obtained through position-sensitive devices (26). The proposed BMFLC algorithm, with $\omega_0 = 2\pi \times 8$, $\omega_n = 2\pi \times 14$, $\Delta\omega = 0.1$

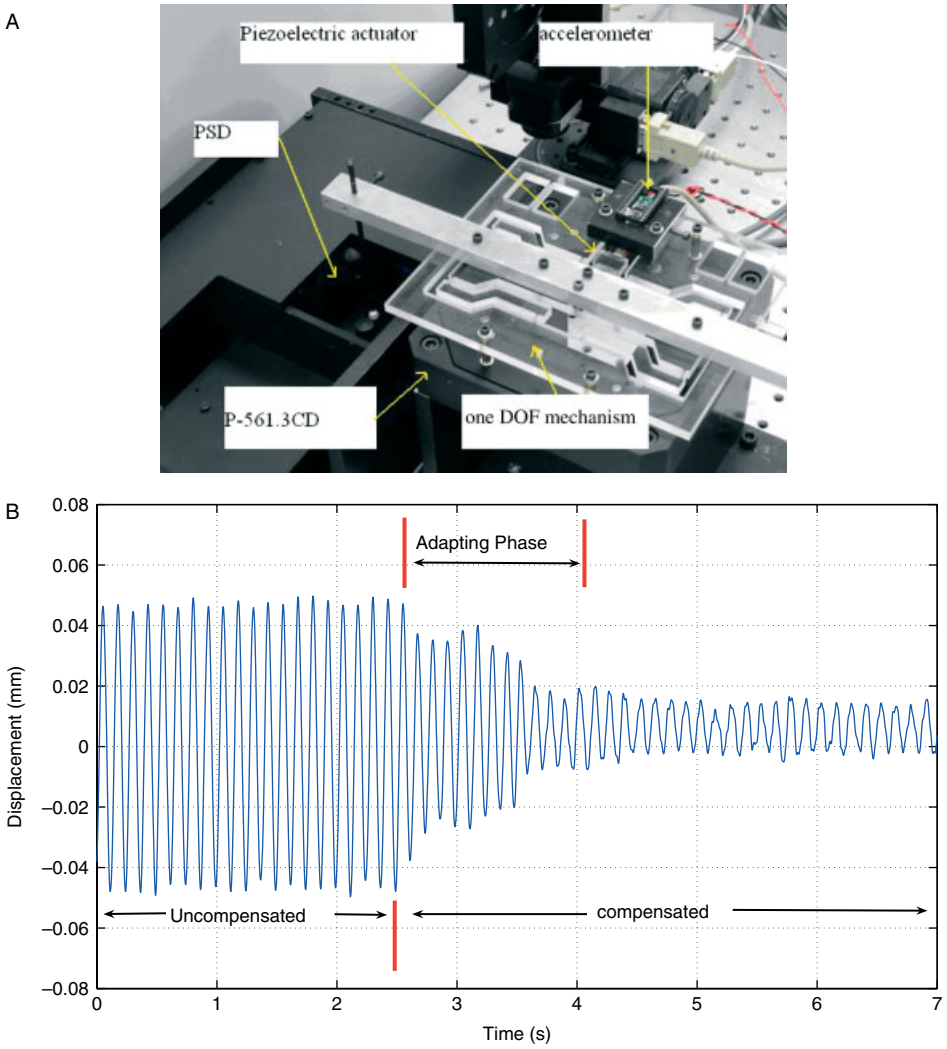

Figure 6. (A) Experimental set-up; (B) compensation with BMFLC

and $\mu = 0.01$, were used for compensation in real-time QNX. The outcome of the experiment is shown in Figure 6B. The compensation was performed after a time gap of 2.5 s after the disturbance input was given. The algorithm adapted for a period of 1.5 s and compensated for the disturbance, as shown in Figure 6B. The RMS value of the motion after compensation dropped to 8.8 μm (by 73.57%).

In order to evaluate the real-time performance for the case of tremor, a known positive tremor signal of a subject recording, as shown in Figure 7A, was given as input to the system. Using BMFLC, the recorded tremor from accelerometers was converted to position and the result is shown in Figure 7A. The dotted line shows the estimated tremor, and error in compensation is shown in Figure 7B. A compensation of 67% was achieved. Most trials showed the settling time to be around 2–3 s. Minimizing the errors in sensing and reducing inevitable delays caused by capacitors would certainly improve the experimental performance. To compare the performance, the WFLC method was implemented in real-time QNX with the following parameters (8): $\mu_0 = 0.002$, $\hat{\mu} = 1 \times 10^{-5}$ and initial guess for the frequency ω_{0_1} was chosen to be 7 Hz. The result can be seen in Figure 7C, D. The tremor motion was compensated by 46%.

To conclude our study, the system was tested with various tremor profiles of several novice subjects and surgeons and the results are tabulated in Table 4. As a surgeon's tremor amplitude is smaller and the frequency components are more distributed than those of novice subjects, a surgeon's tremor compensation is more challenging. Proper band selection is an important factor in achieving better tremor compensation. On average, tremor compensation for surgeons is comparatively lower than that for novice subjects, as shown in Table 4.

Conclusions and Discussion

A study was conducted on the tremor characteristics of several subjects, including surgeons, and revealed that the majority of subjects have tremor distributed in a band with several dominant frequencies. Based on these tremor characteristics, a new algorithm was developed to estimate/filter tremor in a given band of interest. Data recordings of the surgeons were used to

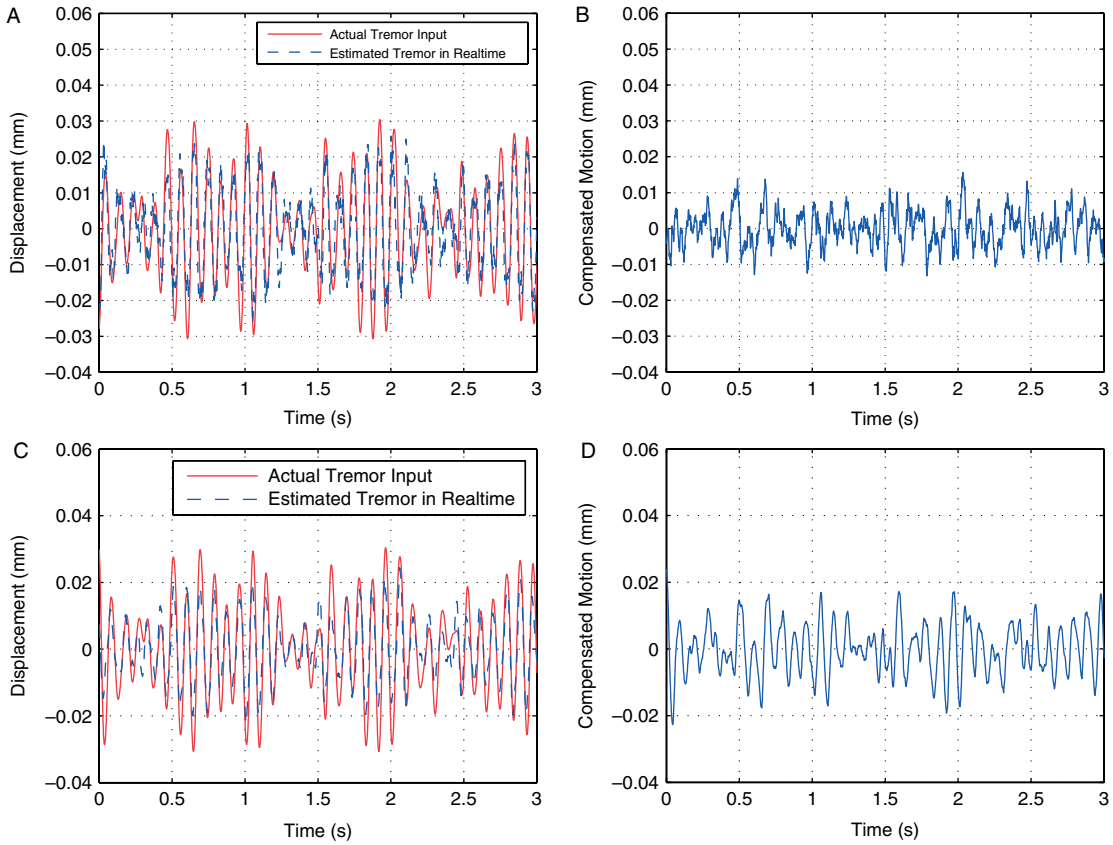

Figure 7. (A) Estimation with BMFLC; (B) compensated motion with BMFLC; (C) estimation with WFLC; (D) compensated motion with WFLC

Table 4. Real-time performance of WFLC and BMFLC

	Average compensation (%)	
Subjects	WFLC	BMFLC
Novice subjects (4 M, 2 F)	48.7	68.4
Surgeons (6 M, 4 F)	43.0	62.8

M, male; F, female.

demonstrate the effectiveness of the proposed algorithm, with which accelerometer data can be used to obtain the position information from the sensed acceleration. Experimental results for 1-DOF compensation of tremor in real time proved the effectiveness of the proposed method compared with WFLC. An average compensation of 66% was achieved with BMFLC, in contrast to 44% with WFLC for surgeons.

As part of our research in developing smart surgical devices such as Micron (7,23) with accelerometers, the algorithms were developed for cancellation of tremor in real time with accelerometers. 3-DOF accelerometers-based sensing to provide tip positions of x, y and z separately is under development. The BMFLC algorithm can be applied for the three axes separately and 3-DOF cancellation of tremor can be achieved. Further research is required to deal with complex gestures involved during microsurgery. An intentional sudden jerk caused by a surgeon is a huge challenge for identification and filtering in real time during microsurgery. Most trials with complex tasks will be performed in future to test the performance of BMFLC.

Acknowledgements

We sincerely thank the surgeons of National University Hospital, Singapore for providing their time in recording the tremor. We specially thank the reviewers for their constructive suggestions, which helped us to improve the quality of the paper. This research was supported by Kyungpook National University Research Fund, 2009.

References

1. Charles S. Dexterity enhancement for surgery. In *Computer Integrated Surgery: Technology and Clinical Applications*, Taylor RH, *et al*. (eds). MIT Press: Cambridge, MA, 1996.
2. Riley P, Rosen M. Evaluating manual control devices for those with tremor disability. *J Rehab Res* 1987; **24**: 99–110.
3. Elble RJ, Koller WC. *Tremor*. John Hopkins University Press: Baltimore, MD, 1985.
4. Harwell RC, Ferguson RL. Physiologic tremor and microsurgery. *Microsurgery* 1983; **4**: 187–192.
5. Humayun MU, Rader RS, Pieramici DJ, *et al*. Quantitative measurement of the effects of caffeine and propranolol on surgeon hand tremor. *Arch Opthalmol* 1997; **115**(3): 371–374.
6. Riviere CN, Gangloff J, De Mathelin M. Robotic compensation of biological motion to enchance surgical accuracy. *Proc IEEE* 2006; **94**(9): 1705–1716.

7. Riviere CN, Radar RS, Thakor N. Adaptive cancelling of physiological tremor for improved precision in microsurgery. *IEEE Trans Biomed Eng* 1998; **45**(7): 839–846.
8. Riviere CN, Thakor N. Modeling and canceling tremor in human-machine interfaces. *IEEE Eng Med Biol* 1996; **15**(3): 29–36.
9. Gonzalez JG, Heredia EA, Rahman T, *et al*. A new approach to suppressing abnormal tremor through signal equalization. Proceedings of the (RESNA) Annual Conference, Vancouver, BC, 1995; 707–709.
10. Morrison S, Keogh J. Changes in the dynamics of tremor during goal-directed pointing. *Hum Movement Sci* 2001; **20**(4–5): 675–693.
11. Timmer J. Modeling noisy time series: physiological tremor. *Int J Bifurc Chaos* 1998; **8**: 1505–1516.
12. Becker BC, Tummala H, Riviere CN. Autoregressive modeling of physiological tremor under microsurgical conditions. In Proceedings of the IEEE 30th Annual Engineering in Medicine and Biology Society (EMBS) Conference, Vancouver, BC, Canada, 2008; 1948–1951.
13. Gonzalez JG, Heredia EA, Rahman T, *et al*. Optimal digital filtering for tremor suppression. *IEEE Trans Biomed Eng* 2000; **47**(5): 664–673.
14. Zhang J, Chu F. Real-time modeling and prediction of physiological hand tremor. In Proceedings of the IEEE International Conference on Acoustics, Speech and Signal Processing, March 2005; vol 5, 645–648.
15. Oppenheim AV, Schaefer RW. *Discrete-time Signal Processing*. Prentice-Hall: Englewood Cliffs, NJ, 2001.
16. Jacobus HN, Riggs AJ, Jacobus CJ, *et al*. Implementation issues for telerobotic hand controllers: human-robot ergonomics. In *Human Robot Interaction*, Rahimi M, Karwowski W (eds). Taylor and Francis: London, 1992.
17. Widrow B, Stearns SD. *Adaptive Signal Processing*. Prentice-Hall: Englewood Cliffs, NJ, 1985.
18. Vaz C, Thakor N. Adaptive Fourier estimation of time-varying evoked potentials. *IEEE Trans Biomed Eng* 1989; **36**(4): 448–455.
19. Vaz C, Kong X, Thakor N. An adaptive estimation of periodic signals using a Fourier linear combiner. *IEEE Trans Signal Process* 1994; **42**(1): 1–10.
20. Riviere CN, Reich SG, Thakor N. Adaptive Fourier modeling for quantification of tremor. *J Neurosci Methods* 1997; **74**: 77–87.
21. Bodson M, Douglas SC. Adaptive algorithms for the rejection of sinusoidal disturbances with unknown frequency. *Automatica* 1998; **33**(12): 2213–2221.
22. Riviere CN, Ang WT, Khosla PK. Toward active tremor canceling in handheld microsurgical instruments. *IEEE Trans Robotics Autom* 2003; **19**(5): 793–800.
23. Ang WT, Riviere CN, Khosla PK. An active hand-held instrument for enhanced microsurgical accuracy. *Med Image Computing Comput Assist Intervent* 2000; **1935**: 878–886.
24. Zhang J, Chu F, Mohammed N. Dsp controller based signal processing of physiological hand tremor. In Proceedings of the American Control Conference, Portland, OR, USA, 2005; 1569–1574.
25. Veluvolu KC, Tan UX, Latt WX, *et al*. Bandlimited multiple Fourier linear combiner for real-time tremor compensation. In IEEE International Conference on Engineering in Medicine and Biology Society, Lyon, France, 2007; 2847–2850.
26. Win TL, Tan UX, Shee CY, *et al*. Design and calibration of an optical micro-motion sensing system for micromanipulation tasks. In IEEE International Conference on Robotics and Automation, Rome, Italy, 2007.
27. Win TL, Tan UX, Veluvolu KC, *et al*. System to access accuracy of micromanipulation. In IEEE International Conference on Engineering in Medicine and Biology Society, Lyon, France, 2007; 5743–5746.
28. Glover J. Adaptive noise cancelling applied to sinusoidal interferences. *IEEE Trans Acoust Speech Signal Process* 1977; **25**(6): 484–491.
29. Tan UX, Veluvolu KC, Latt WT, *et al*. Estimating displacement of periodic motion with inertial sensors. *IEEE Sensors J* 2008; **8**(8): 1385–1388.